6-20-2020

Insights into the adsorption of Pb(II) over trimercapto-s-triazine trisodium salt-modified lignin in a wide pH range

Qiaorui Wang

Chunli Zheng

Fei He

Yuan Yao

Tian C. Zhang

See next page for additional authors

Authors
Qiaorui Wang, Chunli Zheng, Fei He, Yuan Yao, Tian C. Zhang, and Chi He

Chemical Engineering Journal Advances 1 (2020) 100002

Contents lists available at ScienceDirect

Chemical Engineering Journal Advances

journal homepage: www.elsevier.com/locate/ceja

Insights into the adsorption of Pb(II) over trimercapto-s-triazine trisodium salt-modified lignin in a wide pH range

Qiaorui Wang [a], Chunli Zheng [a,b,*], Jianyu Zhang [a], Fei He [a], Yuan Yao [c], Tian C. Zhang [d], Chi He [a,e,*]

[a] Department of Environmental Science and Engineering, Xi'an Jiaotong University, Xi'an 710049, PR China
[b] Key Laboratory of Thermo-Fluid Science and Engineering, School of Energy and Power Engineering, Xi'an Jiaotong University, Xi'an 710049, PR China
[c] WISDRI City Environment Protection Engineering Limited Company, Wuhan, 430205, PR China
[d] Civil Engineering Department, University of Nebraska-Lincoln, Omaha Campus, Omaha, NE 68182-0178, United States
[e] National Engineering Laboratory for VOCs Pollution Control Material & Technology, University of Chinese Academy of Sciences, Beijing 101408, PR China

ARTICLE INFO

Keywords:
Alkaline lignin
Modification
Adsorption
Pb(II)

ABSTRACT

A novel fabrication method for modifying alkaline lignin (AL) was reported, in which trimercapto-s-triazine trisodium salt was used as a modifier to tune surface properties of AL. Molecular structure of modified AL (FAL) was determined by 3D-EEM, synchronous fluorescence, FTIR, ^{13}C MAS NMR and XPS. Two-dimensional correlation spectroscopy and electron localization function demonstrated that both of electrostatic and coordinate bonds formed between these functional groups and Pb(II) at higher pH of 3.0 to 6.0 while only coordinate bond at lower pH of 0.2 to 1.2. The higher the solution pH was, the stronger the adsorption capacity of FAL had. The maximum adsorption capacity (q_m) of Pb(II) was 20.0, 28.2, 65.1 and 73.7 mg/g at pH of 0.2, 1.2, 3.0 and 6.0 (T = 25 °C), respectively. The adsorption performance of FAL towards Pb(II) was better by comparing with other biomass-based materials *via* adsorption amount, equilibrium time as well as simplicity of the synthesized steps. These results improve the understanding of FAL-Pb(II) interaction at the molecular level and facilitate a comprehensive evaluation on the treatment efficiency of FAL.

1. Introduction

Lignin is a class of complex organic polymers and exists in vascular plants and some algae. Next to cellulose, lignin is the second most abundant natural organic materials in the world [1]. The pulp and paper industry discharges lignin as a by-product, with an estimated amount being more than 70 million tons in 2017 [2]. In order to avoid the environmental pollution and make the waste profitable, exploring and developing various ways for lignin utilization has attracted more and more attention. Lignin can be used as fuel, adhesive, lubricant, dispersant, coating and plasticizer [3,4]. Besides, lignin can be used to adsorb heavy metals due to its hydrophobic polymer chain and the existence of several functional groups on its surface, including phenolic hydroxyl (-OH), methoxyl (–OCH_3), aldehyde (R–C=O) and ether (–C–O–C) [5,6]. However, lignin needs to be modified before use in order to increase the specific surface area and introduce more functional groups so that the ability for adsorbing heavy metals is improved [7].

As for the modification methods, three kinds of functional groups including oxygen-, nitrogen- and sulfur-containing [8-10] groups are generally introduced to the skeleton of lignin. For instance, N-acetyl-L-cysteine was used as the modifier to introduce carboxyl groups on the surface of lignin, and the maximal adsorption capacity (q_m) of the modified lignin for Pb(II) and Cu(II) were 55.5 and 68.7 mg/g, respectively [11]. Due to possessing hydroxyl groups, methanol is regarded as a suitable reagent for ornamenting lignin [12]. After modification of lignin, the q_m of Pb(II) was 6.46 mg/g [12]. Methylamine [13], amine [9] and *N*-methylaniline [14] are often used to modify lignin *via* Mannich reaction, in which amino (-NH_2) or imide (-NH) are introduced. Corresponding to the methylamine-modified lignin, the amine-modified lignin and the *N*-methylaniline-modified lignin, the q_m values of Pb(II), Cu(II) and Ag(I) were 60.5, 55.4 and 1556.8 mg/g, respectively. As for the modification of lignin with sulfur-containing functional groups, mercaptan (-SH), sulfonate (-SO_3^-), xanthate (-OCS_2^-) and dithiocarbamate (-CSS^-) are usually introduced. Li et al. [10] prepared a kind of lignin xanthate resin (LXR) by using carbon sulfide (CS_2) as the modifier, and the associated q_m of Pb(II) was 64.9 mg/g, presumably due to the dithiocarbamate group on the surface of LXR. These results demonstrate that after modification, lignin is capable of efficiently removing heavy metals

* Corresponding authors at: Department of Environmental Science and Engineering, Xi'an Jiaotong University, Xi'an 710049, PR China.
E-mail addresses: clzheng@xjtu.edu.cn (C. Zheng), chi_he@xjtu.edu.cn (C. He).

https://doi.org/10.1016/j.ceja.2020.100002
Received 16 April 2020; Received in revised form 19 June 2020; Accepted 20 June 2020

from aqueous solution. However, these reported modification methods have the shortcomings of tedious operating procedures and using several kinds of reagents.

Trimercapto-s-triazine trisodium salt (TMT) is an organic compound with high water solubility (about 540 g/L at 25 °C) [15] and attracts a great deal of attention in terms of coordination chemistry [16]. The 1,3,5-triazine ring constitutes the basic structure of TMT, in which three functional groups of -SH link with C2, C4 and C6 atoms, respectively. The hydrogen atom of -SH is then replaced by Na atom to form -SNa. As TMT contains three N and three S atoms, it is widely used for removing heavy metals such as Pb(II), Cu(II), Cd(II), Ni(II) and Hg(II) from aqueous solution by chelation [17,18]. When approximately 0.3 g/L of TMT was dissolved into 100 mg/L of Cd(II)- and 340 mg/L of Hg(II)-loaded wastewater in the presence of PAC (polyaluminum chloride), precipitation occurred, and the residual concentrations of Cd(II) and Hg(II) were as low as 0.011 mg/L [19] and 0.015 mg/L [20] with the removal efficiencies of 99.9% and 99.8%, respectively. Besides the excellent chelating ability, TMT is cheap and commercially available [21,22]. Therefore, we hypothesized that TMT could be used for lignin modification.

In order to testify such a hypothesis, we prepared a kind of modified lignin and evaluated its adsorption performance for Pb(II) in this study. Lead was selected as the target compound as lignin is regarded as the best low-cost adsorbent for removing aquatic Pb(II) [23]. The molecular structure of the prepared TMT-modified lignin was determined, and its active adsorption sites were determined. To our knowledge, this is the first report on the modification of lignin by using TMT. This work aims at not only providing a novel method for modifying lignin, but also obtaining an adsorbent with good treatment performance towards heavy metals.

2. Experiments

2.1. Materials

Alkaline lignin (AL) with analytical grade was purchased from Tokyo Chemical Industry (Shanghai, China). Trimercapto-s-triazine trisodium salt (TMT, $C_3N_3S_3Na_3$, molecular weight = 243, 15 wt% aqueous solution) was provided by Sigma-Aldrich (America). The analytical reagents of iodine (I_2) and potassium iodide (KI) were brought from Nantong Lingang Chemical Co., Ltd (Nantong, China). Sodium hydroxide (NaOH) and hydrochloric acid (HCl) were supplied by Tianjin Fuyu fine chemical Co., Ltd. (Tianjin, China). Standard solution of $Pb(NO_3)_2$ (1000 μg/mL) was obtained from National Standard Inspection and Certification Co., Ltd (Beijing, China). Ultrapure water was prepared *via* a SPI-11–10T apparatus (Sichuan, China).

2.2. Modification of alkaline lignin

The detailed procedure for AL modification can be found in Text S1 of Supporting Information (SI). In order to testify the success of the modification, the surface property of FAL was characterized and the molecular structure was detected, as shown in Text S2.

2.3. Adsorption and regeneration

The initial concentration of Pb(II) in aqueous solution ranged from 1.0 to 30 mg/L. Adsorption kinetic and isothermal models were established. After adsorption, FAL was regenerated by HCl solution and the reusing ability was evaluated based on a four-adsorption-desorption cycle. The detailed experimental steps were presented in Text S3.

2.4. Insight into the molecular interaction between FAL and Pb(II)

In order to ascertain the active sites for adsorbing Pb(II) as well as sequence the binding affinity of these sites for Pb(II), Fourier transform infrared spectrometer (FTIR) was used to record the adsorption process. The FTIR spectra were then analyzed by using two-dimensional correlation spectroscopy (2D-COS). The molecular bonds between the functional groups of the modified AL and Pb(II) under different pH values were deduced by 2D-COS and the method of electron localization function (ELF) (Text S4).

3. Results and discussion

3.1. Modification of alkaline lignin

The advantages of the method developed in this study for fabricating FAL are as follows: (1) it is easy to operate as shown in Scheme 1 and Text S1; (2) besides AL, four chemical reagents (I_2, KI, TMT and ultrapure water) are needed; and (3) it can be regarded as a relatively economic method as the cost of KI, I_2 and TMT are not high. Hu et al. [24] manufactured a kind of composites, lignin-graft-poly(acrylic acid), in which AL was used as the raw material and six reagents including N,N-dimethylformamide, ammonium persulfate, acrylic acid, N,N-methyl- enebisacryla-mide, acetone and deionized water were needed. Hong et al. [25] used formaldehyde, sodium sulfite, 1,6-dibromo hexane, sodium hydroxide potassium iodide, hexane and deionized water as the reagents to sulfomethylated alkaline lignin. The operational steps described by Hu et al. [24] and Hong et al. [25] are more complicated compared to the procedure shown in Scheme 1. In the synthesis of FAL, the operation just included agitation, centrifugation and vacuum freeze-drying. For the material prepared by Hu et al. [24], besides agitation and centrifugation, nitrogen atmosphere and acetone extraction were needed. In the method developed by Hong et al. [25], reflux, hexane extraction and desalt by ion-exchange resin were required. The method for synthesizing FAL can be regarded as simple and relatively economic.

3.2. Characterization of FAL

Fig. S1A shows the SEM images of AL and FAL, in which AL was composed of relatively large particles with an average diameter of 10 μm while FAL was made up of fine particles with an average diameter of 1 μm. The specific surface areas of AL and FAL were calculated to be 0.089 and 66.05 m^2/g (Fig. S1B), respectively. The average pore diameter of FAL was 13.2 nm, indicating that FAL was of mesoporous structure. Fig. S1C demonstrates that the contents of nitrogen and sulfur increased about 31 and 12 times by modifying AL (0.5%, 2.7%) to FAL (15.6%, 32.6%), respectively. AL is mainly composed of carbon (55.3%), oxygen (22.0%), hydrogen (5.1%) and tiny amounts of nitrogen and sulfur (Fig. S1C). FAL mainly consists of carbon (33.5%), sulfur (32.6%), nitrogen (15.6%) and oxygen (10.5%). Since nitrogen and sulfur are easy to form coordinate bond with heavy metals (coordinate bound: the groups donate their available electron pairs to couple with empty orbitals of metal cations) [26, 27], the prepared FAL should exhibit high adsorption efficiency for Pb(II).

To our best knowledge, reports on the modification of AL by using TMT as the modifier are still rare. Therefore, it is hard to find enough supporting information on the microstructure of FAL. Herein, FTIR, X-ray photoelectron spectroscopy (XPS), ^{13}C magic angle spinning nuclear magnetic resonance spectra (^{13}C MAS NMR), three-dimensional excitation-emission matrix (3D-EEM) and synchronous fluorescence were used in order to deduct the proposed molecular structure of FAL. Steps for the deduction were as follows: (1) the molecular structure of AL used in this study; and (2) the proposed molecular structure of FAL based on the molecular structures of AL and TMT. It was noted here that the molecular structure of TMT has been ascertained as it was purchased as a chemical.

It is well known that lignin has three basic structural units, which are coniferyl alcohol (G), sinapyl alcohol (S) and *p*-coumaryl alcohol (H) (Fig. S2) [28]. Therefore, we need to know which unit the AL used in this study has. Firstly, the peak at E_x/E_m (excitation/emission) of 240/390 nm from the 3D-EEM spectrum (Fig. 1A) and the peak at 1214

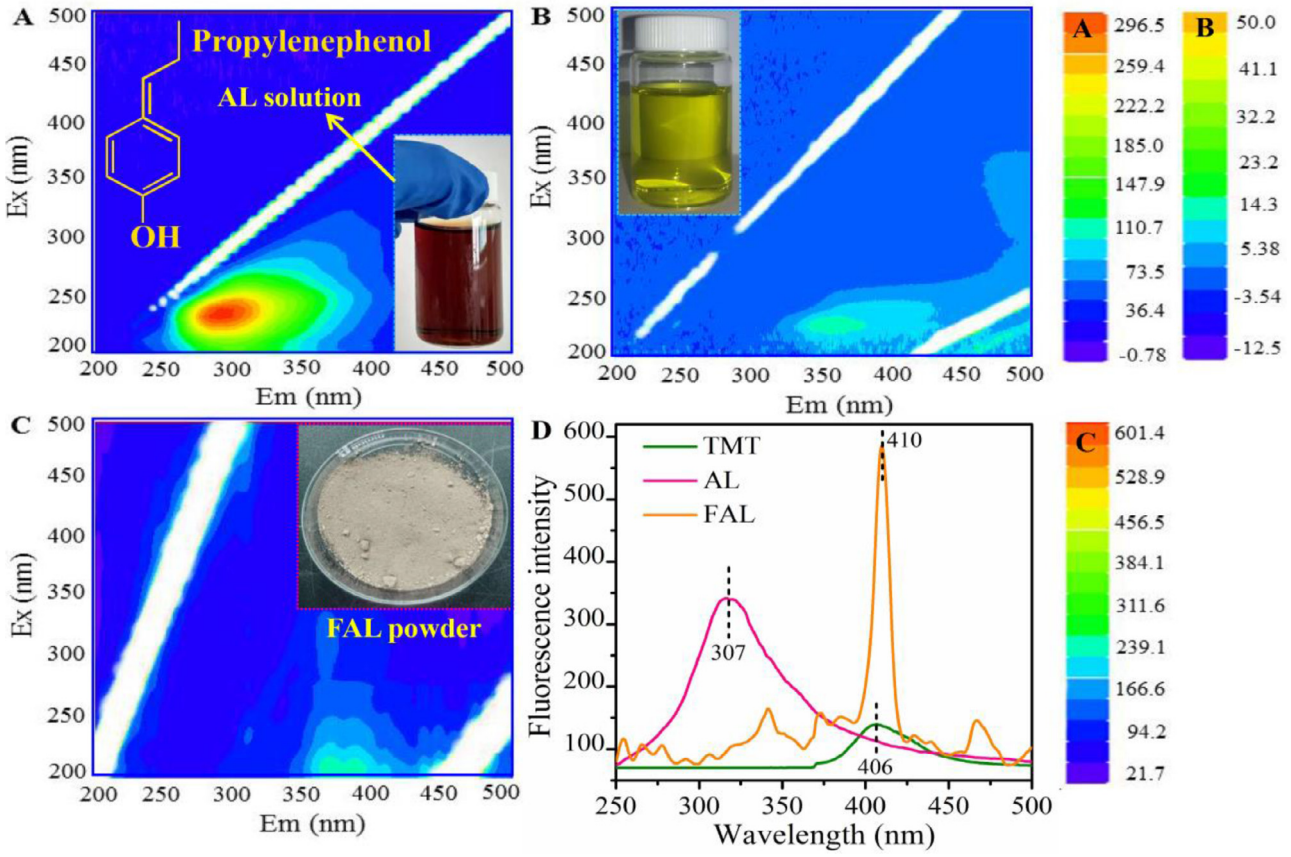

Fig. 1. 3D-EEM fluorescence spectra for (A) AL solution; (B) TMT solution; (C) FAL solid powder; and (D) the synchronal fluorescence spectra of AL solution, TMT solution, and FAL solid powder.

cm^{-1} from the FTIR spectrum (Fig. 2Aa and Table S1) proved the existence of propylenephenol structure. Secondly, the peaks at 2938, 2840 and 1463 cm^{-1} from the FTIR spectrum (Fig. 2Aa and Table S1) as well as the peak at 54.8 ppm from the ^{13}C MAS NMR spectrum (Fig. 2Ba) were attributed to the methoxyl group [29]. Combining the spectral analysis and the images shown in Fig. S2, we hypothesized that the AL used in this paper might have the basic unit of coniferyl alcohol or sinapyl alcohol. Five peaks centered at 1591, 1511, 1265, 1040 and 856 cm^{-1} appeared in Fig. 2Aa, which suggested that the basic structural unit of AL used in this study is coniferyl alcohol (Table S1 and Text S2). The ^{13}C MAS NMR spectra of AL (Fig. 2Ba) also verified this statement as the two peaks at 146.9 and 114.6 ppm were attributed to the C_3 and C_5 in coniferyl alcohol [29]. However, we need to take further investigation on what the functional groups that linked to the three C atoms of propylene of the coniferyl alcohol belong to. As the peaks at 3418, 1650 and 1127 cm^{-1} (Fig. 2Aa and Table S1) were assigned to the groups of O–H [30], conjugated carbonyls group [31] and C–O-R [32], respectively, the proposed molecular structure of AL was finally determined and shown in Fig. 2C.

Fig. 2Bb shows the ^{13}C MAS NMR spectrum of FAL, in which the peaks at 146.9, 114.6 and 54.8 ppm proved the existence of coniferyl alcohol in FAL [32]. The peak at 170.0 ppm was attributed to the carbon atom in the triazine ring of TMT [32]. The peaks at 1471, 1231, 825 and 783 cm^{-1} from the FTIR spectrum (Fig. 2Ac and Table S2) also verified that FAL contained TMT. These results demonstrated that AL reacted with TMT. The reaction mechanism was further explored.

According to the proposed molecular structure of AL shown in Fig. 2C, the functional groups marked 1 to 5 might be the active sites for reaction. It was observed that C–O-R (1128 cm^{-1} in Fig. 2Ac), conjugated carbonyls group (1734 cm^{-1} in Fig. 2Ac and 178.1 ppm in Fig. 2Bb), $-OCH_3$ (2938 and 2840 cm^{-1} in Fig. 2Ac) and -OH (3418 cm^{-1} in Fig. 2Ac) still remained (also see in Table S2 for more details). However, the peak (1214 cm^{-1} in Fig. 2Aa) correspond to phenolic hydroxyl disappeared. These results mean that TMT might react with AL *via* the phenolic hydroxyl group. The peak at 1031 cm^{-1} (Fig. 2Ac), the peak at 410 nm from the synchronous fluorescence spectra (Fig. 1D) and the S 2p peak centered at 165.5 eV from X-ray photoelectron spectroscopy (XPS) (Fig. 3 and Text S2) indicated that the existence of aliphatic sulfoxide [33]. Therefore, the proposed structure of FAL was determined as the one shown in Fig. 2C. It was noted here that the reason why we thought TMT molecule linked with each other *via* the disulphide bond [34] was that the peak at 535 cm^{-1} belonged to the functional group of S-S (Fig. 2Ac and Table S2). Li et al. [22] reported that under the existence of I_2/KI saturated solution TMT and TMT reacts with each other through the formation of S-S bond. The detailed analysis of XPS spectra on FAL was shown in Text S2.

3.3. Adsorption and regeneration

The effect of contact time on the adsorption of Pb(II) over FAL was investigated (Fig. 4A). At the initial concentration of 1 to 30 mg/L, there was no obvious difference in the values of q_t at 40 min and 100 min. All the equilibrium times were determined as 100 min, meaning that the equilibrium time was independent of the initial concentrations of Pb(II). All the values of q_t at 5 min accounted for more than 80% of the equilibrium adsorption amounts (q_e) (Fig. 4A) and all the removal efficiency of Pb(II) was higher than 95% at 100 min (Fig. 4B). These results indicated the adsorption of Pb(II) on FAL was a fast process and an ideal treatment was achieved . Moreover, it was observed that the values of q_t increased with an increase in the initial concentration of Pb(II), indicating that higher Pb(II) concentration improved the driving

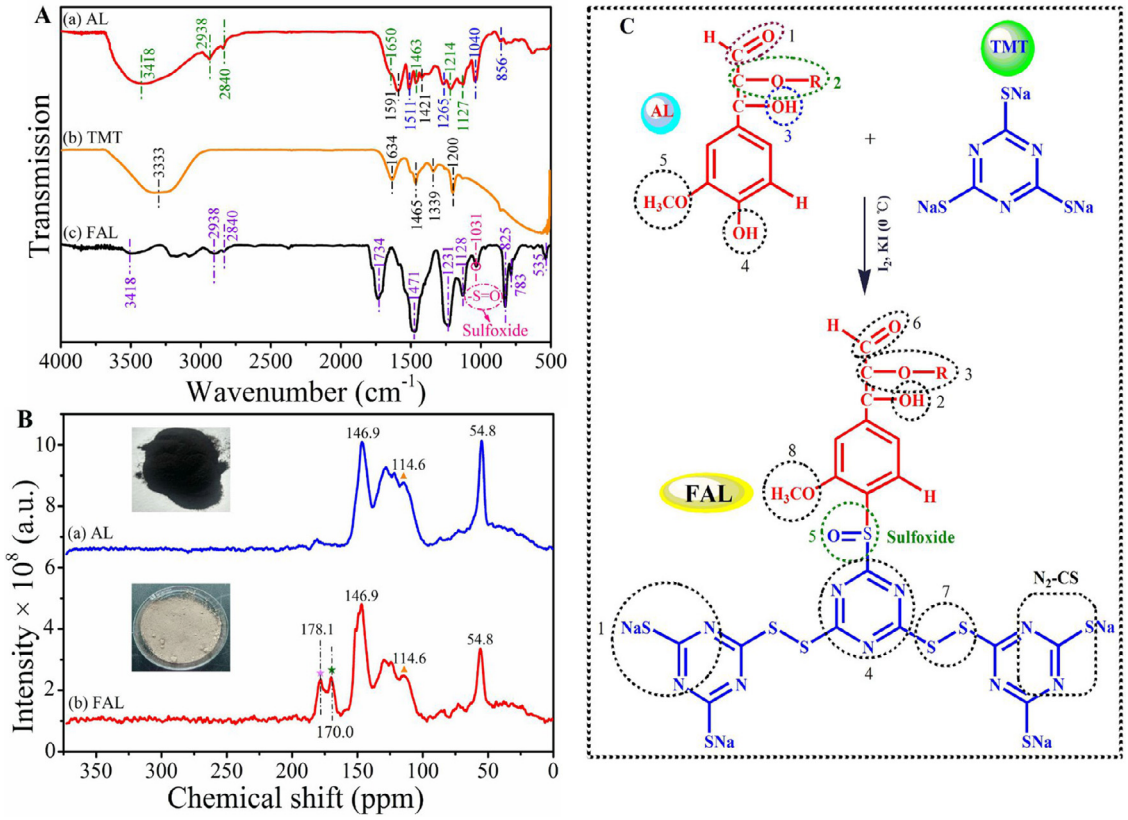

Fig. 2. (A) FTIR spectra of AL powder, TMT solution and FAL powder; (B) ^{13}C MAS NMR spectra of AL and FAL powder; and (C) the deducted molecular structures of AL and FAL.

Table 1
Parameters of the pseudo-first order and pseudo-second order kinetic models for the adsorption of Pb(II) onto FAL at 25 °C and pH of 6.0.

Parameter	Initial concentrations of Pb(II) (mg/L)					
	1	5	10	15	20	30
$q_{e,exp}$ (mg/g)	1.0	4.9	9.8	13.9	19.3	27.9
Pseudo-first-order						
$q_{e,cal}$ (mg/g)	1.7	1.7	1.7	6.2	12.2	18.9
K_1 (1/min)	3.175	0.003	0.003	0.009	0.024	0.022
Δq (%)	1.201	4.776	13.188	3.329	1.281	1.105
R^2	0.0349	0.1348	0.1088	0.3237	0.3526	0.1169
Pseudo-second-order						
$q_{e,cal}$ (mg•min)	1.0	4.9	9.8	13.9	19.5	27.8
K_2 (g/(mg•min))	6.730	2.229	4.196	1.786	0.560	1.192
Δq (%)	0.043	0.096	0.045	0.112	0.256	0.149
R^2	0.9998	0.9999	0.9999	0.9998	0.9987	0.9999

force to overcome the mass transfer-resistant barrier between solid and aqueous phases.

Both the pseudo-first-order (Fig. S4A) and pseudo-second-order (Fig. 4C) kinetic models were used to fit the data shown in Fig. 4A. Table 1 demonstrated that the pseudo-second-order kinetic model fitted better. It can be seen from Fig. 4C and Table 1, all the values of correlation coefficient (R^2) for the linear plots of t/q_t against time from the pseudo-second-order model were consistent and close to unity. Moreover, the values of Δq were lower and $q_{e,cal}$ better agreed with $q_{e,exp}$. These results showed that the adsorption of Pb(II) on FAL was a chemisorption process, involving valency forces through sharing or exchange of electrons between sorbent and sorbate [35,36]. Fig. S4B presents the intra-particle plots for the adsorption of Pb(II) on FAL at different initial concentrations. The values of the rate constant and intercept were given in Table S3. It was observed all the linear portions of the plots over the entire time range did not pass through the origin. This result demonstrated that the adsorption rate of Pb(II) might be affected by both of the bulk diffusion and the intra-particle diffusion [37]. To further verify the real control step, Boyd's film-diffusion model was used and the results were shown in Fig. S3C and Table S4. It can be concluded that the adsorption rate of Pb(II) on FAL was controlled by film diffusion [37].

Fig. 4D and Fig. S4 show that the Freundlich model (R^2 = 0.9512) described the isothermal data better than the Langmuir model (R^2 = 0.9139), suggesting that the uptake of Pb(II) by FAL was multilayer adsorption [38]. The value of q_m for Pb(II) adsorption on FAL at pH = 6.0 was calculated to be 73.7 mg/g. The Langmuir constant K_L ($0 < K_L < 1$) and Freundlich constant ($1 < n < 10$) further implied that the adsorption process was favorable [38].

Different concentrations of HCl solution were used as the solvent to extract the adsorbed Pb(II) from the surface of FAL, in which 120 min was determined as the equilibrium time and 0.2 mol/L was proved to

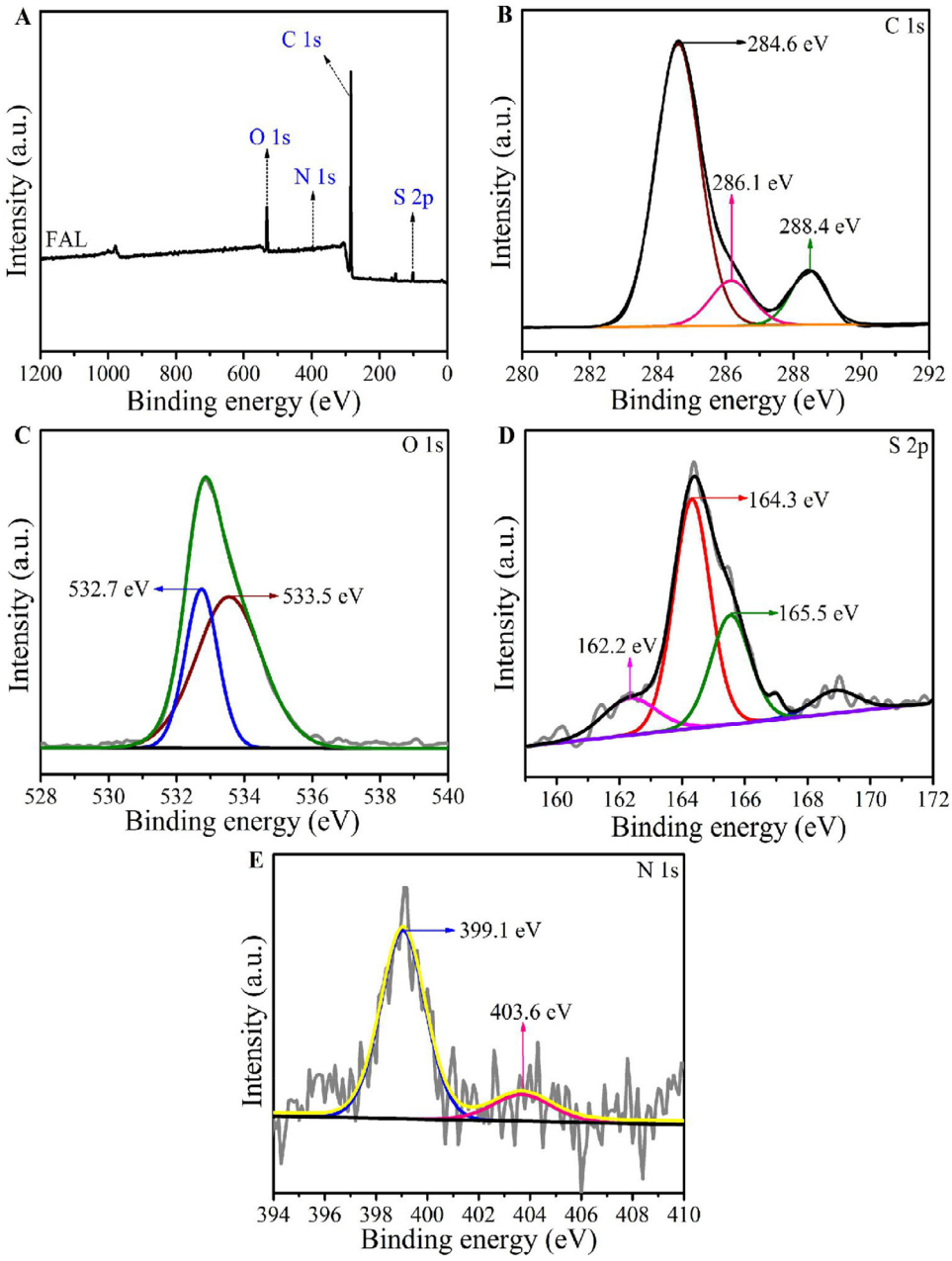

Fig. 3. (A) Full scan survey of XPS spectra for FAL; (B) C 1 s spectra; (C) O 1 s spectra; (D) S 2p spectra and (E) N 1 s spectra.

be the optimal concentration of HCl based on the removal efficiency of Pb(II) (Fig. S5A). Four adsorption-desorption cycles were operated, in which the initial concentration of Pb(II) was set at 15 mg/L (Fig. S5B). It was found that the removal efficiency of Pb(II) were 94%, 90%, 89%, 85% and 83% corresponding to fresh FAL, regenerated FAL at cycle 1, cycle 2, cycle 3 and cycle 4, respectively.

3.4. Insight into the molecular interaction between FAL and Pb(II)

According to the molecular structure of FAL shown in Fig. 2C, we hypothesized that the functional groups marked 1 to 8 might be the active sites for the adsorption of Pb(II) as they contained oxygen, sulfur and nitrogen atoms [26]. In order to testify such a hypothesis, the adsorption of Pb(II) on FAL at different pH values (0.2, 1.2, 3.0 and 6.0) was recorded by using FTIR and the results were shown in Fig. 5. As the precipitation of Pb(II) occurs at pH ≥ 7.2, the solution pH in this study was adjusted at ≤ 6.0 so that the interference of lead hydroxide precipitation was avoided. As the pH_{pzc} of FAL was measured to be 1.2 (Fig. 6B, insert), the surface of FAL would become positively, zero or negatively charged when the solution pH was lower, equivalent to, or higher than 1.2. The FTIR spectra (Fig. 5) were analyzed by using the technology of 2D-COS (Fig. S7 and Tables S5–8). It was found that the functional groups marked 1 to 7 except the methoxyl group took part in the adsorption when the solution pH ranged from 0.2 to 6.0. These results suggested that no matter what kind of charges that the surface of FAL carried, these seven functional groups worked well. Jin et al. [39] prepared a kind of 5-sulfosalicylic acid modified lignin, which contained the functional group of $-SO_3H$ just like aliphatic sulfoxide in FAL. It was found that the exchange of electrons or sharing of valence forces between Pb(II) and $-SO_3H$ happened. Coordinated bond between Zn(II) ions and S-O/S=O was described when the hydroxylated and sulphonated biochars derived from pulp and paper sludge were used as the sorbent [40]. Generally speaking, the methoxyl group was an active site for adsorbing Pb(II) when other kinds of modified AL served as

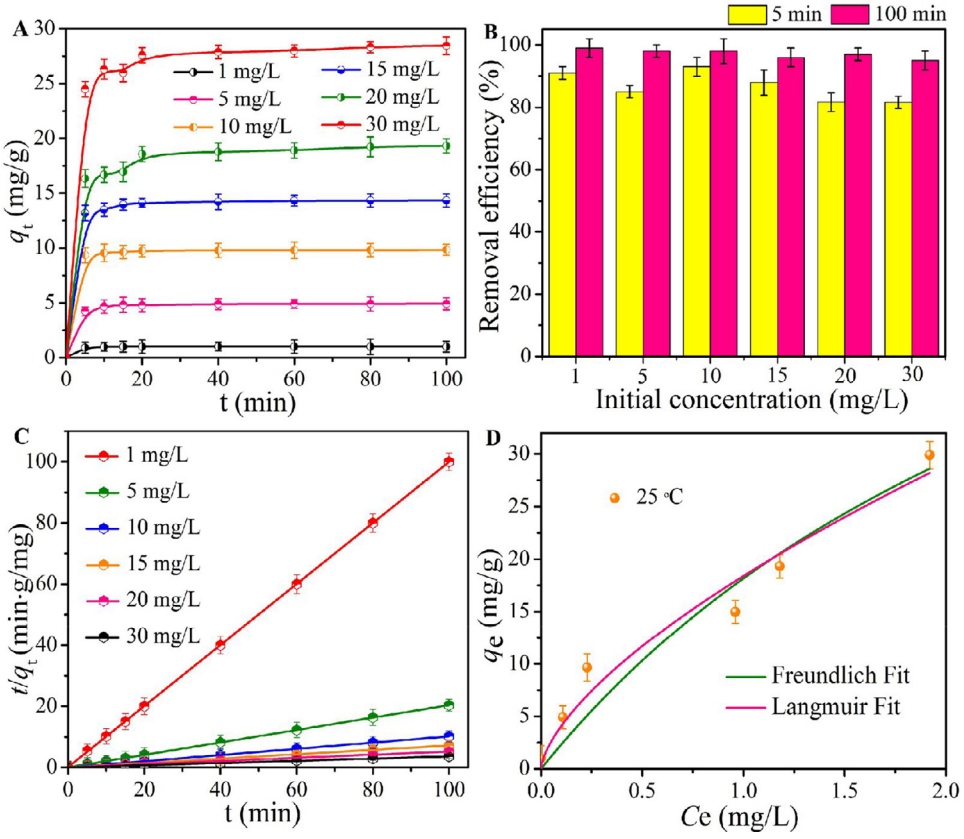

Fig. 4. (A) Effect of contact time on the adsorption of Pb(II) on FAL; (B) the removal efficiency of Pb(II) at 5 min and 100 min corresponding to initial concentrations of 1 to 30 mg/L; (C) simulated plots of the pseudo-second order kinetics; and (D) adsorption isotherm for Pb(II) on FAL (temperature = 25 °C, pH = 6.0, FAL = 1.0 g/L, reaction time = 100 min).

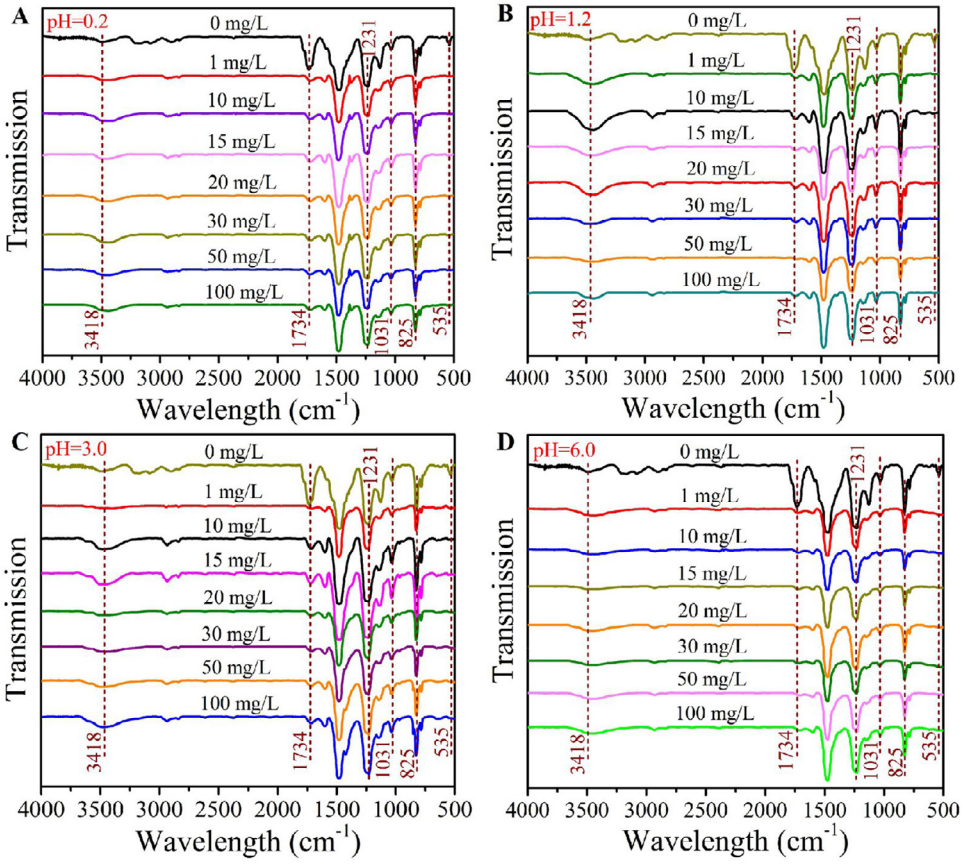

Fig. 5. FTIR spectra of Pb(II) adsorbed on FAL at pH of (A) 0.2, (B) 1.2, (C) 3.0 and (D) 6.0.

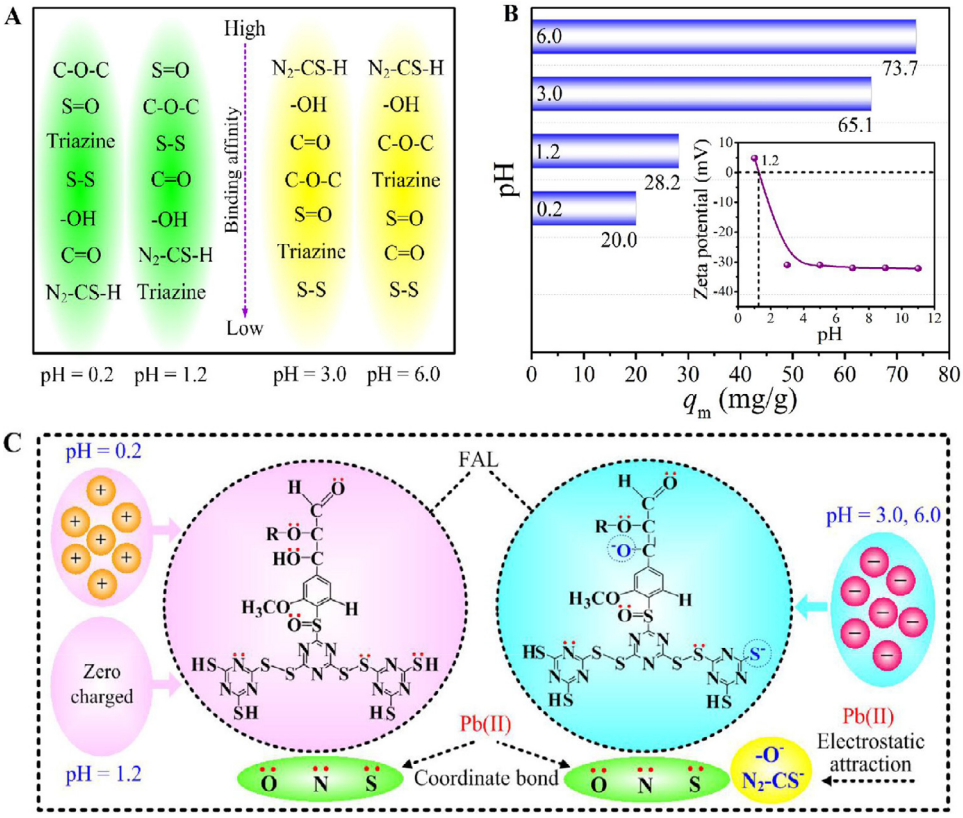

Fig. 6. (A) Binding affinities of the seven functional groups for Pb(II) at different pH values; (B) the values of q_m at different pH values; and (C) molecular insights into the adsorption of Pb(II) at different pH values. *: It was noted here that at low pH of 0.2 and 1.2, there might be thione thiol equilibrium in TMT not sodium ions are on sulfurs.

the sorbent [41,42]. However, in FAL such a group did not work during the adsorption process. The reason was that its exposure to Pb(II) might not be enough.

The binding affinity of the seven functional groups for Pb(II) was sequenced and the results were shown in Fig. 6A. N_2–CS–H and –OH exhibited stronger binding affinity than other functional groups at pH of 3.0 or 6.0, in which the surface of FAL was negatively charged. According to the molecular structure of FAL, N_2–CS-H and –OH possibly underwent dissociation to form N_2–CS^- and $-O^-$ who contributed to the generation of electrostatic bond between FAL and Pb(II) (Fig. 6C). As for other functional groups, they probably reacted with Pb(II) *via* coordinate bond (the oxgen-contianing, sulfur-contianing and nitrogen-contianing groups donate electron pairs from O, N and S atoms to couple with empty orbitals of metal cations) (Fig. 6C) [27,43]. Once the solution pH was adjusted to 1.2 or 0.2, N_2–CS-H and –OH almost exhibited the lowest binding affinity for Pb(II). The possible reason for such a reversion was that the surface of FAL was neurally or positively charged under pH of 1.2 or 0.2 so that only coordinate bond occurred between FAL and Pb(II) [47] (Fig. 6C). At the pH values of 1.2 and 0.2, C–O–C and S=O exhibited the highest binding affinity for Pb(II).

Fig. 6B shows that the best adsorption performance was achieved at pH of 6.0, followed by 3.0, 1.2 and 0.2 based on the values of q_m. As mentioned above, the surface of FAL carries negative charges under pH of 3.0 and 6.0 while positive charges under pH of 0.2, suggesting that the electrostatic attraction/electrostatic repulsion between FAL and Pb(II) exists under pH of 3.0–6.0/0.2. The electrostatic repulsion impedes the attachment of Pb(II) to the surface of FAL. Furthermore, lower pH value means that more amounts of proton exist in solution; thus, the competition between Pb(II) and proton for binding with the active adsorption sites is fiercer. This analysis might explain why FAL presented the highest or lowest adsorption capacity at pH of 6.0 or 0.2, respectively. According to the aforementioned results, three main conclusions could be drawn: (1) both electrostatic attraction and coordinate bond contributed to the adsorption of Pb(II) when the solution pH was higher than the pH_{pzc} (1.2) of FAL; (2) only coordinate bond contributed to the adsorption of Pb(II) when the solution pH was equivalent to or lower than the pH_{pzc} (1.2) of FAL; and (3) FAL can be used for removing Pb(II) from aqueous solution at a wide pH range of 0.2 to 6.0; however, FAL preferred to a relatively alkaline condition.

The atomic electronic populations of ELF can be used to identify the type of molecular interaction [44,45]. When the value of bond polarity index is close to 0, the type of bond can be classified as homopolar (covalent) bond; while close to 1 for idealized ionic bond [45,46]. Fig. 7A and Fig. 7B show the seven active adsorption sites of FAL, in which the functional groups of *C* = *O*, C–O–R, –OH, O=S, S–S, triazine ring and N_2–CS–H was marked as 1, 2, 3, 4, 5, 6 and 7, respectively. The atomic electronic populations describes the molecular interaction between the seven functional groups from 1 to 7 and Pb(II) were recorded as V_1 (S, Pb), V_2 (O, Pb), V_3 (O, Pb), V_4 (N, Pb), V_5 (O, Pb), V_6 (O, Pb) and V_7 (S, Pb) basins. At pH of 0.2 and 1.2 (Fig. 7C), the atomic electronic populations of V_1 (S, Pb), V_2 (O, Pb), V_3 (O, Pb), V_4 (N, Pb), V_5 (O, Pb), V_6 (O, Pb) and V_7 (S, Pb) basins equaled to (0.100 e, 0.618 e), (2.982 e, 5.547 e), (5.846 e, 4.930 e), (0.004 e, 0.001 e), (6.253 e, 4.421 e), (5.934 e, 7.080 e) and (1.573 e, 1.664 e), respectively. Base on the values of atomic electronic populations of V_1 (S, Pb), V_2 (O, Pb), V_3 (O, Pb), V_4 (N, Pb), V_5 (O, Pb), V_6 (O, Pb) and V_7 (S, Pb), the corresponding bond polarity index values of $P_{1(S,Pb)}$, $P_{2(O,Pb)}$, $P_{3(O,Pb)}$, $P_{4(N,Pb)}$, $P_{5(O,Pb)}$, $P_{6(O,Pb)}$ and $P_{7(S,Pb)}$ were calculated to be 0.72, 0.30, 0.09, 0.60, 0.17, 0.09 and 0.03, respectively. Fig. 7D gives the data on the atomic electronic populations of V_1 (S, Pb), V_2 (O, Pb), V_3 (O, Pb), V_4 (N, Pb), V_5 (O, Pb), V_6 (O, Pb) and V_7 (S, Pb) basins at the solution pH of 3.0 and 6.0. Therefore, the bond polarity index values of $P_{1(S,Pb)}$, $P_{2(O,Pb)}$, $P_{3(O,Pb)}$, $P_{4(N,Pb)}$, $P_{5(O,Pb)}$, $P_{6(O,Pb)}$ and $P_{7(S,Pb)}$ were 0.94, 1.0, 0.09, 0.60, 0.17, 0.09 and 0.03, respectively. The calculation methods were the same as those described by Berski et al. [45]. and Raub et al.[46].. As $P_{1(S,Pb)}$ and $P_{2(O,Pb)}$ at pH of 3.0 and 6.0 were closed to 1, it can be concluded that the functional groups of N_2–CS–H and -OH dissociated as N_2–CS^- and $-O^-$, then combined with Pb(II) *via* electrostatic attraction. The other five groups

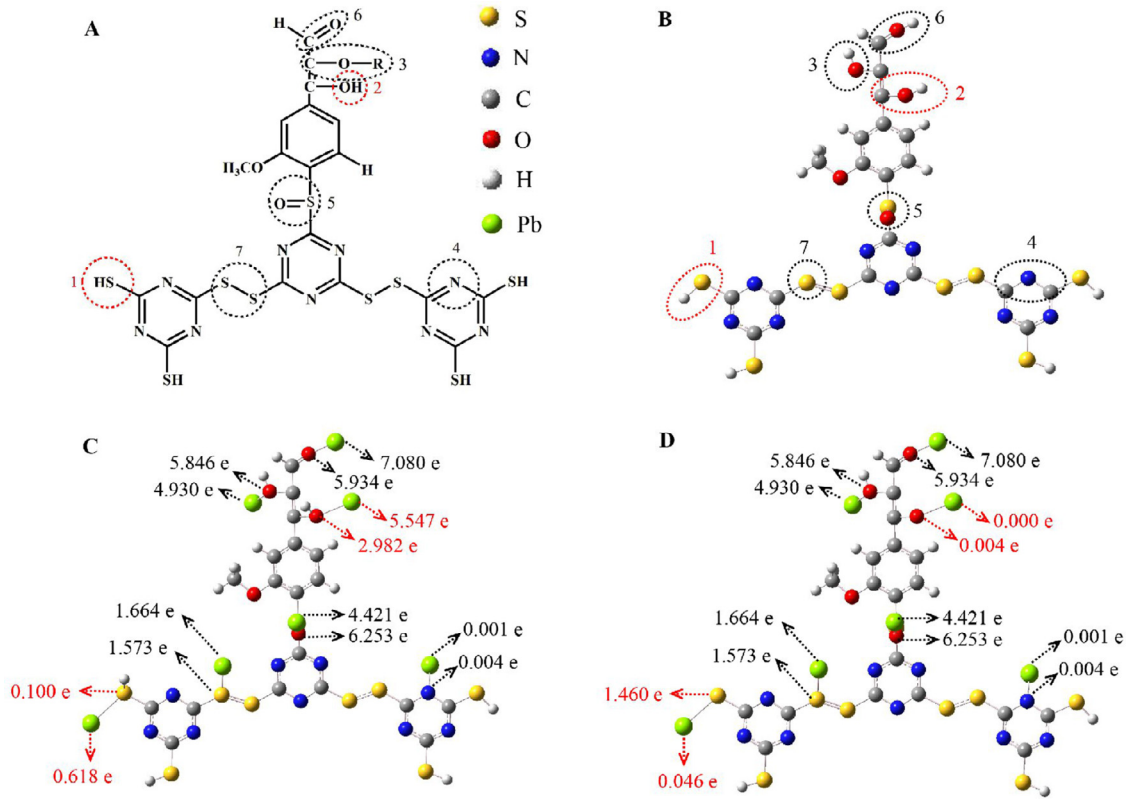

Fig. 7. (A) and (B) The active adsorption sites of FAL for Pb(II); (C) ELF analysis of FAL-Pb(II) complexes at pH of 0.2 and 1.2 and (D) ELF analysis of FAL-Pb(II) complexes at pH of 3.0 and 6.0.

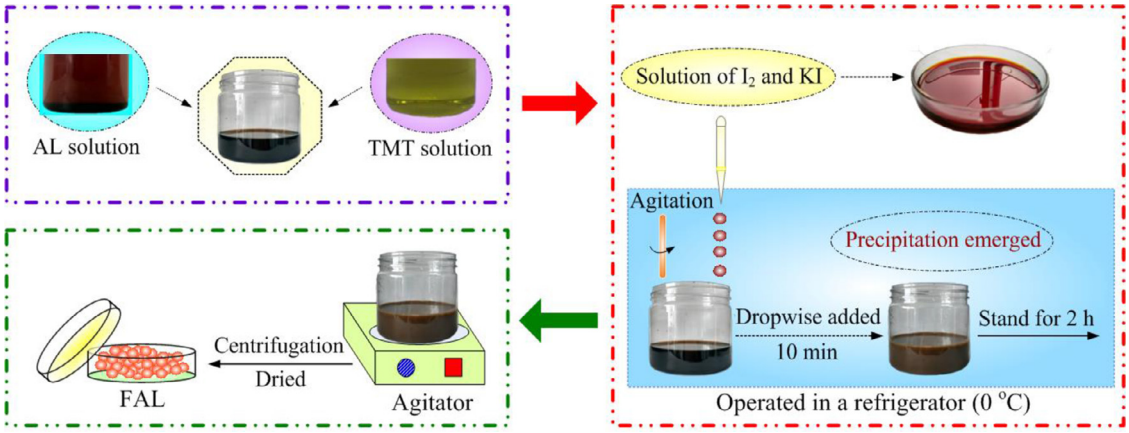

Scheme 1. Synthesis steps of FAL.

of *C* = *O*, C–O–R, O=S, S–S and triazine ring for Pb(II) were more easier to form coordinate bonds. At pH of 0.2 and 1.2, it can be concluded that the coordinate bonds were more likely to be formed between all the seven groups and Pb(II). This result is a further verification of the predicted results described in Fig. 6.

In natural water, the dissolved organic materials (DOMs) consist of humic acid (HA) [48]. Moreover, HA is one of the biodegrading products from plant and animal biomass [49]. The functional groups of phenolic (-OH), carboxylic (-COOH) and amine (-NH_2) carried by HA are thought to be the most active adsorption sites for binding with Pb(II) and other heavy metals [48,50,51]. Town and Leeuwen pointed out that both electrostatic and coordinate bonds contribute to the adsorption of Pb(II) [52], which is similar to the adsorption mechanism of FAL. Just like FAL, increase in the solution pH lead to the increase in the adsorption amount of HA to Pb(II) when the pH value was in the range of 2.5 to 5.0 [48].

3.5. Comparison between FAL and reported sorbents

In order to evaluate the adsorption capacity of FAL for Pb(II) comprehensively, two series of sorbents were selected and shown in Table 2 and Table S9, respectively. Various lignin-based materials were presented in Table 2, in which lignin was used as the raw material just like our work and different modification methods were applied. As lignin belongs to biomass, it is also necessary to know how FAL behaved among the sorbents derived from various biomasses (Table S9). In Table 2, it was found that the values of q_m for the lignin-based nanotrap (LBNT) and surface functionalized porous lignin (SFPL) were al-

Table 2
Comparing the adsorption capacity of FAL towards Pb(II) with other lignin-based adsorbents.

No.	Sorbents	q_m (mg/g)	$q_{m\ (other\ sorbents)}/q_{m(FAL)}$	t [a] (min)	$t_{(other\ sorbents)}/t_{(FAL)}$	pH	Temperature (°C)	*Ref.*
1	FAL	73.7	/	100	/	6.0	25	This work
2	LBNT[b]	324.4	4.40	720	7.2	6.0	25	[53]
3	SFPL[c]	188.0	2.55	180	1.8	5.0	25	[7]
4	Aminated epoxy-lignin	72.5	0.98	90	0.9	6.0	30	[9]
5	HACH[d]	66.26	0.90	180	1.8	/	/	[54]
6	AML[e]	60.5	0.82	140	1.4	6.0	25	[13]
7	TiO_2-SiO_2/lignin hybrid	59.9	0.81	180	1.8	5.0	20	[55]
8	ASL[f]	53.8	0.73	120	1.2	6.0	25	[56]
9	LBA[g]	42.0	0.57	180	1.8	6.0	25	[57]
10	SSAL[h]	39.3	0.53	4500	45	5.8	45	[38]
11	TiO_2/lignin hybrid	35.7	0.48	180	1.8	5.0	20	[55]
12	LMS[i]	33.9	0.46	200	2	6.0	25	[58]
13	MSL[j]	20.0	0.27	360	3.6	5.0	27	[59]
14	SRL[k]	12.7	0.17	120	1.2	6.0	28	[60]

[a] Equilibrium time;.
[b] Lignin-based nano-trap;.
[c] Surface functionalized porous lignin;.
[d] Humic acid-treated coconut (cocos nucifera) husk;.
[e] Methylamine modified alkaline lignin;.
[f] Sulfomethylation and amination modified alkaline lignin;.
[g] Lignin-triazole;.
[h] 5-Sulfosalicylic acid modified lignin;.
[i] Alkaline lignin modified with poly(ethylenimine);.
[j] Modified soda lignin;.
[k] Sulfonated resinified lignin.

most 5 and 3 times higher than that of FAL, respectively. However, the times of reaching adsorption equilibrium for LBNT and SFPL were 7.2 and 1.8 times longer than that of FAL, respectively. When the initial concentration of Pb(II) was 10 mg/L or 20 mg/L, the values of K_2 (the pseudo-second-kinetic-order rate constant) for LBNT or SFPL were 0.005 and 0.004 g/(mg•min), respectively [7,53], while that for FAL under 10 mg/L was 4.196 g/(mg•min) (Table 2). It was noted here under the similar operation temperature and similar initial concentration level, the value of K_2 can be used to compare the adsorption rate of different sorbents for a defined sorbate [35].

Moreover, the synthesis methods and the reagents' toxicity used for the preparation of LBNT and SFPL were more complicated and higher compared to FAL, respectively. To manufacture LBNT, several toxic chemicals such as CS_2, formaldehyde, amine, Span80 and diethylenetriamine were used. The chemicals used in the preparation of SFPL were almost the same as those used in LBNT. The operational steps for LBNT and SFPL include condensation reflux and temperature control. On the contrary, making FAL needs three reagents besides ultrapure water, of which only iodine is toxic while the toxicity of KI and TMT are low, and the procedure is much easier compared to that of making LBNT and SFPL.

Table S9 shows the adsorption capacity of 30 biomass-based sorbents for Pb(II), including cellulose, chitosan and activated carbon. Sorbents 2 to 4 have a higher q_m than FAL does. However, the values of K_2 for sorbents 2 to 4 were 0.0001, 0.001 and 0.002 g/(mg•min) when the initial concentrations of Pb(II) were 100, 20 and 20 mg/L, respectively. These results demonstrated that the adsorption rate of FAL (4.196 g/(mg•min) under 10 mg/L) for Pb(II) was several orders of magnitude higher than that of sorbents 2 to 4. Sorbents 5 to 31 have a lower q_m and longer equilibrium time than that of FAL. These results suggest that FAL be a promising material for purification of Pb(II)-loaded wastewater as its treatment performance and fabrication method were higher and easier than other lignin-based and biomass-based materials.

4. Conclusions

In this paper a novel method for modifying alkaline lignin was developed, in which three kinds of reagents were used in the entire modifying process, i.e., KI, I_2 and TMT. TMT is cheap and easily available. Moreover, the modification process is simple, safe, and relatively economic. The molecular structure of modified alkaline lignin (FAL) was deduced based on the technologies of 3D-EEM, synchronous fluorescence, FTIR and ^{13}C MAS NMR and XPS. According to FAL's molecular structure, the functional groups served as the active adsorption sites were determined. By using two-dimensional correlation spectroscopy (2D-COS) and ELF, the molecular interactions (electrostatic or coordinate bond or both) between the functional groups and Pb(II) at different pH conditions were analyzed. The adsorption capacity of FAL for Pb(II) was compared with other biomass-based materials from the viewpoints of adsorption amount, adsorption rate as well as simplicity and economic cost of the synthesis step. This paper not only provides an easily-operational and relatively economic method for lignin modification but also establishes an approach to analyzing the associated molecular interactions between the sorbent and the sorbate. FAL can be regarded as a promising material with high application potential, which warrants future studies on optimizing FLAL for real-world applications.

Declaration of Competing Interest

The authors declare that they have no known competing financial interests or personal relationships that could have appeared to influence the work reported in this paper.

Acknowledgments

This work was financially supported by the National Natural Science Foundation of China (21876139, 21922606), the Key R&D Program of Shaanxi Province (2019SF-253, 2019SF-244, 2019ZDLSF05-05-02), and the Shaanxi Natural Science Fundamental Shaanxi Coal Chemical Joint Fund (2019JLM-14). The authors gratefully acknowledge the supports from K.C. Wong Education Foundation and Instrument Analysis Center of Xi'an Jiaotong University, as well as appreciate the editor and reviewers for their professional work and valuable comments.

Supplementary materials

Supplementary material associated with this article can be found, in the online version, at doi:10.1016/j.ceja.2020.100002.

References

[1] S. Laurichesse, L. Averous, Chemical modification of lignins: towards biobased polymers, Prog. Polym. Sci. 39 (2014) 1266–1290.

[2] N. Supanchaiyamat, K. Jetsrisuparb, J.T.N. Knijnenburg, D.C.W. Tsang, A.J. Hunt, Lignin materials for adsorption: current trend, perspectives and opportunities, Bioresour. Technol. 272 (2019) 570–581.

[3] V.K. Thakur, M.K. Thakur, P. Raghavan, M.R. Kessler, Progress in green polymer composites from lignin for multifunctional applications: a review, ACS Sustain. Chem. Eng. 2 (2014) 1072–1092.

[4] C.Z. Li, X.C. Zhao, A.Q. Wang, G.W. Huber, T. Zhang, Catalytic Transformation of lignin for the production of chemicals and fuels, Chem. Rev. 115 (2015) 11559–11624.

[5] Y. Zhou, J.P. Zhang, X.G. Luo, X.Y. Lin, Adsorption of Hg(II) in aqueous solutions using mercapto-functionalized alkali lignin, J. Appl. Polym. Sci. 131 (2014) 1–9.

[6] X.J. He, J.J. Xie, Y. Wei, S. Li, K. Huang, X.Q. Han, H.Y. Zhang, Preparation of super-absorbents composites from kaolin/sodium lignosulfonate-g-AA-AM, Sci. Silvae. Sin. 47 (2011) 134–138 (*in Chinese*).

[7] Z.L. Li, D. Xiao, Y.Y. Ge, S. Koehler, Surface-functionalized porous lignin for fast and efficient lead removal from aqueous solution, ACS Appl. Mater. Inter. 7 (2015) 15000–15009.

[8] F.B. Liang, Y.L. Song, C.P. Huang, Y.X. Li, B.H. Chen, Synthesis of novel lignin-based ion-exchange resin and its utilization in heavy metals removal, Ind. Eng. Chem. Res. 52 (2013) 1267–1274.

[9] X.L. Liu, H.X. Zhu, C.R. Qin, J.H. Zhou, J.R. Zhao, S.F. Wang, Adsorption of heavy metal ion from aqueous single metal solution by aminated epoxy-lignin, Bioresources 8 (2013) 2257–2269.

[10] Z.L. Li, Y. Kong, Y.Y. Ge, Synthesis of porous lignin xanthate resin for Pb^{2+} removal from aqueous solution, Chem. Eng. J. 270 (2015) 229–234.

[11] C. Jin, X.Y. Zhang, J.N. Xin, G.F. Liu, J. Chen, G.M. Wu, T. Liu, J.W. Zhang, Z.W. Kong, Thiol-ene synthesis of cysteine-functionalized lignin for the enhanced adsorption of Cu(II) and Pb(II), Ind. Eng. Chem. Res. 57 (2018) 7872–7880.

[12] N. Liu, S.F. Wang, H.X. Zhu, X.L. Liu, Sequential extraction of lignin from sugarcane bagasse: characterization and application in the Pb(II) adsorption, J. Biobased Mater. Bioenergy 13 (2019) 550–556.

[13] Y.Y. Ge, Q.P. Song, Z.L. Li, A Mannich base biosorbent derived from alkaline lignin for lead removal from aqueous solution, J. Ind. Eng. Chem. 23 (2015) 228–234.

[14] Q.F. Lu, J.J. Luo, T.T. Lin, Y.Z. Zhang, Novel lignin-poly(N-methylaniline) composite sorbent for silver ion removal and recovery, ACS. Sustain. Chem. Eng. 2 (2014) 465–471.

[15] K.R. Henke, D. Robertson, M.K. Krepps, D.A. Atwood, Chemistry and stability of precipitates from aqueous solutions of 2,4,6-trimercaptotriazine, trisodium salt, nonahydrate (TMT-55) and mercury (II) chloride, Water Res. 34 (2000) 3005–3013.

[16] K.R. Henke, J.C. Bryan, M.P. Elless, Structure and powder diffraction pattern of 2,4,6-trimer-capto-s-triazine, trisodium salt ($Na_3S_3CSN_3 \bullet 9H_2O$), Powder Differ. 12 (1997) 7–12.

[17] G. Andreottola, M. Cadonna, P. Foladori, G. Gatti, F. Lorenzi, P. Nardelli, Heavy metal removal from winery wastewater in the case of restrictive discharge regulation, Water Sci. Technol. 56 (2007) 111–120.

[18] M.M. Matlock, K.R. Henke, D.A. Atwood, D. Robertson, Aqueous leaching properties and environmental implications of cadmium, lead and zinc trimercaptotriazine (TMT) compounds, Water Res. 35 (2001) 3649–3655.

[19] M. Chen, Z. Liu, L.Y. Lin, L.M. Man, Y.Y. Lu, C.Z. Dai, Removal of cadmium from wastewater using 2,4,6-trimercapo-s-triazine trisodium, Hydrometallur. China 34 (2015) 1–4 (in Chinese).

[20] W.Y. Lü, S.Y. Liu, X.T. Wang, Y.J. Sun, L.C. Nengzi, Q.W. Fu, Treatment of gas field wastewater with high mercury concentration using heavy metal chelator TMT-15, Environ. Protect. Chem. Ind. 35 (2015) 459–463 (*in Chinese*).

[21] N. Tang, C.G. Niu, X.T. Li, C. Liang, H. Guo, L.S. Lin, C.W. Zheng, G.M. Zeng, Efficient removal of Cd^{2+} and Pb^{2+} from aqueous solution with aminoand thiol-functionalized activated carbon: isotherm and kinetics modeling, Sci. Total Environ. 635 (2018) 1331–1344.

[22] X.P. Li, C.Q. Bian, X.J. Meng, F.S. Xiao, Design and synthesis of an efficient nanoporous adsorbent for Hg^{2+} and Pb^{2+} ions in water, J. Mater. Chem. A. 4 (2016) 5999–6005.

[23] Q.X. Yao, J.J. Xie, J.X. Liu, H.M. Kang, Y. Liu, Adsorption of lead ions using a modified lignin hydrogel, J. Polym. Res. 21 (2014) 1–16.

[24] L.Q. Hu, L. Dai, R. Liu, C.L. Si, Lignin-graft-poly (acrylic acid) for enhancement of heavy metal ion biosorption, J. Mater Sci. 52 (2017) 13689–13699.

[25] N.L. Hong, W. Yu, Y.Y. Xue, W.M. Zeng, J.H. Huang, W.Q. Xie, X.Q. Qiu, Y. Li, A novel and highly efficient polymerization of sulfomethylated alkaline lignins via alkyl chain cross-linking method, Holzforschung 70 (2016) 297–304.

[26] Y.Y. Ge, Z.L. Li, Application of lignin and its derivatives in adsorption of heavy metal ions in water: a review, ACS Sustain. Chem. Eng. 6 (2018) 7181–7192.

[27] D. Wu, Y.G. Wang, Y. Li, Q. Wei, L.H. Hu, T. Yan, R. Feng, L.G. Yan, B. Du, Phosphorylated chitosan/$CoFe_2O_4$ composite for the efficient removal of Pb(II) and Cd(II) from aqueous solution: adsorption performance and mechanism studies, J. Mol. Liq. 277 (2019) 181–188.

[28] B.M. Upton, A.M. Kasko, Strategies for the conversion of lignin to high-value polymeric materials: review and perspective, Chem. Rev. 116 (2016) 2275–2306.

[29] E.I. Evstigneyev, A.S. Mazur, A.V. Kalugina, A.V. Pranovich, A.V. Vasilyev, Solid-state C-13 CP/MAS NMR for alkyl-o-aryl bond determination in lignin preparations, J Wood Chem. Technol. 38 (2018) 137–148.

[30] Y. Liu, T.J. Hu, Z.P. Wu, G.M. Zeng, D.L. Huang, Y. Shen, X.X. He, M.Y. Lai, Y.B. He, Study on biodegradation process of lignin by FTIR and DSC, Environ. Sci. Pollut. Res. 21 (2014) 14004–14013.

[31] L.P. Xiao, Z. Lin, W.X. Peng, T.Q. Yuan, F. Xu, N.C. Li, Q.S. Tao, H. Xiang, R.C. Sun, Unraveling the structural characteristics of lignin in hydrothermal pretreated fibers and manufactured binderless boards from Eucalyptus grandis, Sustain. Chem. Process. 2 (2014) 9–21.

[32] T.G. Geng, S.N. Ye, Z.M. Zhu, W.Y. Zhang, Triazine-based conjugated microporous polymers with N,N,N',N'-tetraphenyl-1,4-phenylenediamine, 1,3,5-tris(diphenylamino)-benzene and 1,3,5-tris[(3-*methylphenyl*)-*phenylamino*]benzene as the core for high iodine capture and fluorescence sensing of o-nitrophenol, J. Mater. Chem. A. 6 (2018) 2808–2816.

[33] Y.C. Yang, X.X. Tao, N. Xu, L.Q. Luo, Feasibility study on the FTIR characterization of sulfur-containing groups in coal, China Sciencepaper 10 (2015) 2110–2116 (*in Chinese*).

[34] R.S. Vishwanath, S. Kandaiah, Metal ion-containing $C_3N_3S_3$ coordination polymers chemisorbed to a copper surface as acid stable hydrogen evolution electrocatalysts, J. Mater. Chem. A. 5 (2017) 2052–2065.

[35] Q.R. Wang, C.L. Zheng, Z.X. Shen, Q. Lu, C. He, T.C. Zhang, J.H. Liu, Polyethyleneimine and carbon disulfde co-modifed alkaline lignin for removal of Pb^{2+} ions from water, Chem. Eng. J. 359 (2019) 265–274.

[36] W.L. Zhang, R. Fu, L. Wang, J.W. Zhu, J.T. Feng, W. Yan, Rapid removal of ammonia nitrogen in low-concentration from wastewater by amorphous sodium titanate nano-particles, Sci. Total Environ. 668 (2019) 815–824.

[37] B. Tang, Y.W. Lin, P. Yu, Y.B. Luo, Study of aniline/ε-caprolactam mixture adsorption from aqueous solution onto granular activated carbon: kinetics and equilibrium, Chem. Eng. J. 187 (2012) 69–78.

[38] Y.Z. Zhang, S.C. Lin, J.Q. Qiao, D. Kolodynska, Y.M. Ju, M.W. Zhang, M.F. Cai, D.Y. Deng, D.D. Dionysiou, Malic acid-enhanced chitosan hydrogel beads (mCHBs) for the removal of Cr(VI) and Cu(II) from aqueous solution, Chem. Eng. J. 353 (2018) 225–236.

[39] Y.Q. Jin, C.M. Zeng, Q.F. Lu, Efficient adsorption of methylene blue and lead ions in aqueous solutions by 5-sulfosalicylic acid modified lignin, Int. J. Biol. Macromol. 123 (2019) 50–58.

[40] N. Chaukura, W. Gwenzi, N. Mupatsi, D.T. Ruziwa, C. Chimuka, Comparative adsorption of Zn^{2+} from aqueous solution using hydroxylated and sulphonated biochars derived from pulp and paper sludge, Water, Air, Soil Pollut 228 (2017) 1–12.

[41] A.B. Albadarin, A.H. Al-Muhtaseb, N.A. Al-laqtah, G.M. Walker, S.J. Allen, M. Ahmad, Biosorption of toxic chromium from aqueous phase by lignin: mechanism, effect of other metal ions and salts, Chem. Eng. J. 169 (2011) 20–30.

[42] M. Brdar, M. Šćiban, A. Takaći, T. Dosenovic, Comparison of two and three parameters adsorption isotherm for Cr(VI) onto kraft lignin, Chem. Eng. J. 183 (2012) 108–111.

[43] N. Chaukura, W. Gwenzi, N. Mupatsi, D.T. Ruziwa, C. Chimuka, Comparative adsorption of Zn^{2+} from aqueous solution using hydroxylated and sulphonated biochars derived from pulp and paper sludge, Water, Air, Soil Pollut. 228 (2017) 1–12.

[44] T. Lu, F.W. Chen, Multiwfn: a multifunctional wavefunction analyzer, J. Comput. Chem. 33 (2012) 580–592.

[45] S. Berski, Z. Latajka, Quantum chemical topology: the electronic structure of the alkaline nitrites MONO (M = Li, Na, K) studied by means of topological analysis of the electron localization function, Int. J. Quantum Chem. 110 (2010) 1890–1900.

[46] S. Raub, G. Jansen, A quantitative measure of bond polarity from the eletron localization function and the theory of atoms in molecules, Theor. Chem. Acc. 106 (2001) 223–232.

[47] D. Wu, Y.G. Wang, Y. Li, Q. Wei, L.H. Hu, T. Yan, R. Feng, L.G. Yan, B. Du, Phosphorylated chitosan/CoFe2O4 composite for the efficient removal of Pb(II) and Cd(II) from aqueous solution: adsorption performance and mechanism studies, J. Mol. Liq. 277 (2019) 181–188.

[48] A.G. Liu, R.D. Gonzalez, Modeling adsorption of copper(II), cadmium(II) and lead(II) on purified humic acid, Langmuir 16 (2000) 3902–3909.

[49] R.P. Chen, Y.L. Zhang, L.F. Shen, X.Y. Wang, J.Q. Chen, A.J. Ma, W.M. Jiang, Lead(II) and methylene blue removal using a fully biodegradable hydrogel based on starch immobilized humic acid, Chem. Eng. J. 268 (2015) 348–355.

[50] J. Xiong, L.K. Koopal, W.F. Tan, L.C. Fang, M.X. Wang, W. Zhao, F. Liu, J. Zhang, L.P. Weng, Lead binding to soil fulvic and humic acids: nICA-donnan modeling and XAFS spectroscopy, Environ. Sci. Technol. 47 (2013) 11634–11642.

[51] J. Hizal, R. Apak, W.H. Hoell, Modeling competitive adsorption of copper(II), lead(II), and cadmium(II) by kaolinite-based clay mineral/humic acid system, Environ. Prog. Sustain. Energy 28 (2009) 493–506.

[52] R.M. Town, H.P. Leeuwen, Intraparticulate speciation analysis of soft nanoparticulate metal complexes. The impact of electric condensation on the binding of $Cd^{2+}/Pb^{2+}/Cu^{2+}$ by humic acids, Phys. Chem. Chem. Phys. 18 (2016) 10049–10058.

[53] D. Xiao, W. Ding, J.B. Zhang, Y.Y. Ge, Z.J. Wu, Z.L. Li, Fabrication of a versatile lignin-based nano-trap for heavy metal ion capture and bacterial inhibition, Chem. Eng. J. 358 (2019) 310–320.

[54] B.G.N. Sewwandi, M. Vithanage, S.S.R.M.D. Wijesekara, M.I.M. Mowjood, S. Hamamoto, K. Kawamoto, Adsorption of Cd(II) and Pb(II) onto humic acid-treated coconut (cocos nucifera) husk, J. Hazard. Toxic Radioact. Waste 18 (2014) 04014001.

[55] L. Klapiszewski, K. Siwinska-Stefanska, D. Kolodynska, Preparation and characterization of novel TiO_2/lignin and TiO_2-SiO_2/lignin hybrids and their use as functional biosorbents for Pb(II), Chem. Eng. J. 314 (2017) 169–181.

[56] Y.Y. Ge, Z.L. Li, Y. Kong, Q.P. Song, K.Q. Wang, Heavy metal ions retention by bi-functionalized lignin: synthesis, applications, and adsorption mechanisms, J. Ind. Eng. Chem. 20 (2014) 4429–4436.
[57] C. Jin, X. Zhang, J. Xin, G. Liu, G. Wu, Z. Kong, J. Zhang, Clickable synthesis of 1,2,4-triazole modifed lignin-based adsorbent for the selective removal of Cd(II), ACS Sustain. Chem. Eng. 5 (2017) 4086–4093.
[58] Y.Y. Ge, L. Qin, Z.L. Li, Lignin microspheres: an effective and recyclable natural polymer-based adsorbent for lead ion removal, Mater. Des. 95 (2016) 141–147.
[59] M.N.M. Ibrahim, W.S.W. Ngah, M.S. Norliyana, W.R.W. Daud, M. Rafatullah, O. Sulaiman, R. Hashim, A novel agricultural waste adsorbent for the removal of lead (II) ions from aqueous solutions, J. Hazard. Mater. 182 (2010) 377–385.
[60] B.O. Ogunsile, M.O. Bamgboye, Biosorption of Lead (II) onto soda lignin gels extracted from Nypa fruiticans, J. Environ. Chem. Eng. 5 (2017) 2708–2717.